Time Accurate Finite Difference Method for Performance Prediction of a Silencer with Mean Flow and Nonlinear Incident Wave

Changjeon Hwang*
Rotorcraft Development Division, Korea Aerospace Research Institute, 45, Eoeun, Yuseong, Daejeon 305-333, Korea
Duck Joo Lee
Department of Aerospace Engineering, Korea Advanced Institute of Science and Technology, 373-1, Kusong, Yuseong, Daejeon 305-701, Korea
Kang Seog Chae
Small Engine Development Team, GM Daewoo Auto & Technology, 199-1, Chungchun, Bupyeong, Incheon 403-714, Korea

Transmission losses of various reactive silencers are predicted, using a time accurate finite difference method. The numerical scheme is the 3rd order upwind scheme for axisymmetric Euler equations. Main advantage of the present method is that it can simulate linear and nonlinear wave propagation phenomena in a flow field directly with minimum numerical oscillation errors. The special treatments of incident wave condition, i.e. multiple harmonics of the transparent acoustic condition are applied to the transmission loss prediction for calculation efficiency. For the validation of the present approach, circular expansion chamber silencers without mean flow and an exponential pipe with mean flow are simulated in case of linear incident wave. The computed transmission losses have quite good agreements with those of the others. The nonlinear incident wave case is also investigated to check the usefulness of this method. The periodic N wave is clearly captured without numerical oscillation errors, and the insertion losses of two different incident frequencies are compared.

Key Words : Silencer Performance, Transmission Loss, Nonlinear Incident Wave, Mean Flow, Euler Equations, Finite Difference Method

1. Introduction

Various numerical methods have been developed to describe the acoustic field in silencer and to predict the silencer performance. The calculation and analysis of sound attenuation characteristics are the foundation of designing reactive silencers. It is practically important in optimal silencer design to predict the acoustic performance of a silencing system accurately with various effects such as complex geometry, higher order mode, nonlinear waves, temperature gradient, and arbitrary mean flow gradient. Not only the convection, but also refraction, generation, and scattering of acoustic energy are known as the mean flow effects. The numerical methods developed so far can be just partly considered those kinds of mean flow effects.

The transfer matrix method based on plane wave theory has been widely used in one dimensional analyses of the silencer, and transfer ma-

* Corresponding Author,
E-mail : chwang@kari.re.kr
TEL : +82-42-860-2363; **FAX** : +82-42-860-2006
Rotorcraft Development Division, Korea Aerospace Research Institute, 45, Eoeun, Yuseong, Daejeon 305-333, Korea. (Manuscript **Received** March 23, 2006; **Revised** October 20, 2006)

trices for various types of silencer elements also have been obtained (Munjal, 1987a). Various semi-analytic methods using the eigen function series and the matched boundary condition are developed considering the higher order modes and/or axial mean flow gradient (Munjal, 1987b ; Åbom, 1990 ; Kim et al., 1990 ; Easwaran and Munjal, 1992). Boundary element method and finite element method in frequency domain is also applied to the silencer performance prediction (Ji et al., 1994 ; Tsuji et al., 2002). Time accurate methods such as a method of characteristics and FDM (Kim and Lee, 2001) have been introduced to simulate the acoustic field. Time accurate approach produces its solution in the same way as that of experiment, so that it can be helpful to understand the physical phenomena, especially transient state and nonlinear physics in the space and time domain.

Objectives of this study are to establish the prediction procedure using a time accurate finite difference method of Euler equations for the silencer performance analyses and then to validate the accuracy and usefulness. The rotational, inviscid and compressible flow including acoustic waves can be directly simulated by using Euler equations. The advantages of this approach rely on the direct consideration of arbitrary mean flow gradients, higher order modes, linear and nonlinear waves, flow-acoustic interaction and even complex geometry effects. The numerical schemes for Euler equations are extended straightforwardly to the Navier-Stokes equations also. In this study, the conventional higher order upwind scheme, so-called Roe's upwind scheme (Hirsch, 1990) is applied as starting point for this approach. In this study, the multiple harmonics of transparent acoustic conditions (Hwang and Lee, 1995) for the incident wave conditions and the calculation process for transmission loss prediction are newly applied.

To validate the present approach, two different shapes of circular expansion chamber silencer are solved. Both cases are considering linear incident waves and no mean flow gradient. However, the extended inlet and outlet tubes are considered in one of both cases. Then the transmission loss calculation in an exponential pipe with complex mean flow gradient is carried out with two different mean flow Mach number conditions. Finally the nonlinear incident wave case is investigated to check the usefulness of this approach.

2. Governing Equations and Numerical Algorithm

The strong conservative forms of unsteady compressible axisymmetric Euler equations in generalized coordinates are employed as the governing equations in this study. The 2nd order Runge-Kutta method is used for the temporal discretization of the governing equation, and the 3rd order MUSCL (Monotone Upwind Schemes for Conservation Laws) type Roe's upwind finite difference, i.e. node based formulation is applied for the spatial discretization (Hirsch, 1990). The tangency condition is applied along the internal wall surface. The nonreflecting boundary condition for outlet and acoustic source condition for inlet are employed to simulate the wave propagation in a silencer.

2.1 Nonreflecting boundary conditions

Thompson's boundary condition (Thompson, 1990) is applied for nonreflecting boundary condition. At the inlet or outlet boundary of $\xi=$ const as shown in Fig. 1, the wave can be considered as one dimensional so that,

$$\partial_{\tau_{\hat{\xi}}}\hat{\boldsymbol{W}}+\hat{\Lambda}\partial_{\hat{\xi}}\hat{\boldsymbol{W}}=0 \tag{1}$$

where

$$\begin{aligned}\delta\hat{\boldsymbol{W}}&=(\delta W_1,\ \delta W_2,\ \delta W_3,\ \delta W_4)^T\\&=(\delta\rho-\delta p/c^2,\ \delta q_t,\ \delta p+\rho c\delta q_n,\ \delta p-\rho c\delta q_n)^T\\ \hat{\Lambda}&=\mathrm{Diag}(\lambda_1,\lambda_2,\lambda_3,\lambda_4)\\&=\mathrm{Diag}(q_n,q_n,q_n+c,q_n-c)\end{aligned} \tag{2}$$

$$q_n=\hat{\xi}_x u+\hat{\xi}_y v,\ q_t=\hat{\xi}_y u-\hat{\xi}_x v$$

$$\hat{\xi}_x=\xi_x/\sqrt{\xi_x^2+\xi_y^2},\ \hat{\xi}_y=\xi_y/\sqrt{\xi_x^2+\xi_y^2}$$

where ρ is a gas density. u and v are the gas velocity components in x and y respectively, and c is local speed of sound. Eq. (1) can be decomposed into incoming and outgoing parts based on the directions of the eigenvalue, λ_i,

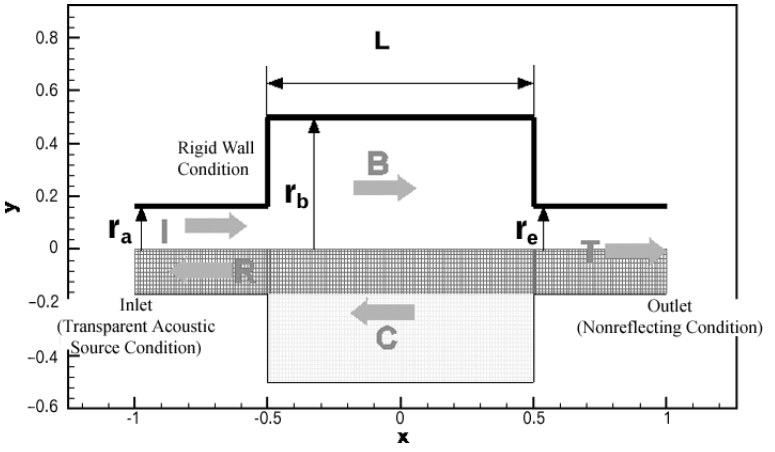

Fig. 1 Computational domain and schematic drawing for a circular expansion chamber silencer without extended inlet/outlet ($L/r_b=2,\ r_b/r_a=3,\ r_a/r_e=1$)

$$\partial_{\tau_\xi}\hat{\boldsymbol{W}}|_{in}+\hat{\Lambda}|_{in}\partial_\xi\hat{\boldsymbol{W}}=0 \tag{3}$$

$$\partial_{\tau_\xi}\hat{\boldsymbol{W}}|_{out}+\hat{\Lambda}|_{out}\partial_\xi\hat{\boldsymbol{W}}=0 \tag{4}$$

For example, the eigenvalues λ_1,λ_2 and λ_3 correspond to the incoming part and λ_4, to the outgoing part at the outlet. To be a nonreflecting boundary, $\hat{\Lambda}|_{in}$ is set to zero. So, the values of incoming characteristic variables remain unchanged at the boundaries. So, we can rewrite Eqs. (3) and (4) as,

$$\partial_{\tau_\xi}\hat{\boldsymbol{W}}|_{in}=0 \tag{5}$$

$$\partial_{\tau_\xi}\hat{\boldsymbol{W}}|_{out}=-\hat{\Lambda}|_{out}\partial_\xi\hat{\boldsymbol{W}} \tag{6}$$

In Eq. (6), $-\hat{\Lambda}|_{out}\partial_\xi\hat{\boldsymbol{W}}$ are calculated by one sided difference. Then Eqs. (5) and (6) are integrated in time along with the interior values.

2.2 Transparent acoustic source conditions

The term, $\partial_{\tau_\xi}\hat{\boldsymbol{W}}|_{in}$ in Eq. (3) should be specified by the specific value using appropriate relations to make the incoming wave equivalent to a sound source. First, we use the plane wave relations, which is valid in stationary or uniformly moving medium :

$$\begin{aligned}&\partial_{\tau_\xi}p=\varepsilon\omega\cos(\omega\tau)\\&\partial_{\tau_\xi}q_n=\pm\partial_{\tau_\xi}p/\rho c\\&\qquad(+,\text{ right going},\ -,\text{ left going})\\&\partial_{\tau_\xi}q_t=0\\&\partial_{\tau_\xi}\rho=\partial_{\tau_\xi}p/c^2\end{aligned} \tag{7}$$

At the inlet, Eqs. (5) and (6) can be rewritten as,

$$\begin{aligned}&\partial_{\tau_\xi}W_1|_{in}=\partial_{\tau_\xi}\rho-\partial_{\tau_\xi}p/c^2=0\\&\partial_{\tau_\xi}W_2|_{in}=\partial_{\tau_\xi}q_t=0\\&\partial_{\tau_\xi}W_3|_{in}=\partial_{\tau_\xi}p+\rho c\partial_{\tau_\xi}q_n\neq0\\&\partial_{\tau_\xi}W_4|_{in}=-\lambda_4\partial_\xi W_4\end{aligned} \tag{8}$$

At the outlet

$$\begin{aligned}&\partial_{\tau_\xi}W_1|_{out}=-\lambda_1\partial_\xi W_1\\&\partial_{\tau_\xi}W_2|_{out}=-\lambda_2\partial_\xi W_2\\&\partial_{\tau_\xi}W_3|_{out}=-\lambda_3\partial_\xi W_3\\&\partial_{\tau_\xi}W_4|_{out}=\partial_{\tau_\xi}p-\rho c\partial_{\tau_\xi}q_n\neq0\end{aligned} \tag{9}$$

These source conditions are called by transparent acoustic source (Hwang and Lee, 1995), which permits the nonreflecting property for outgoing wave at the boundary on the source side. This condition is useful for the prediction of transmission loss directly. The reflected wave, $\boldsymbol{R}$ is not reflected at the inlet again if this condition is applied at the inlet as shown in Fig. 1. To get a transmission loss more efficiently, the multiple harmonic source condition in Eq. (10) is employed, so that the transmission loss with respect to incident wave frequencies can be predicted not from the multiple calculations of each single incident wave frequency, but from only one calculation of multiple harmonic incident waves.

$$\partial_{\tau_\xi}p=\varepsilon\sum_{i=1}^{i\max}(i2\pi\Delta f)\cos\{(i2\pi\Delta f)\tau\} \tag{10}$$

3. Results and Discussion

In this study, the length and time scales are nondimensionalized by the characteristic length of $\tilde{L}$ and $\tilde{L}/\tilde{c}_o$, where $\tilde{c}_o$ is the speed of sound in the flow at rest. The angular frequency, $\tilde{\omega}$, which is the dimension of inverse time, is nondimensionalized by $(\tilde{L}/\tilde{c}_o)^{-1}$. Here, tilde, $\sim$ means a dimensional quantity. The frequency is defined as $\tilde{\omega}=2\pi\tilde{f}$. If $\tilde{L}$ is 0.1(m) and $\tilde{c}_o$ is 340(m/sec), the nondimensional $f=0.5$ is about 1.7(kHz). If the peak amplitude of acoustic source, ε is 0.00001, it corresponds to about 90 dB in SPL (sound pressure level). If ε is 0.1, it is about 170 dB in SPL.

3.1 Linear incident wave without meanflow

The characteristic length is chosen as the length of expansion chamber, L as shown in Fig. 1. The transmission loss is defined as below

$$TL=10\log_{10}(|\mathbf{I}|/|\mathbf{T}|)^2 \tag{11}$$

where $\boldsymbol{I}, \boldsymbol{T}$ are peak amplitudes of the incident and the transmitted waves at the corresponding frequency. $\boldsymbol{I}$ is the known value and $\boldsymbol{T}$ is calculated using FFT of the time history of acoustic pressure at outlet.

The circular expansion chamber silencer with no extended inlet and outlet as shown in Fig. 1 is analyzed firstly. Grid system consists of 2 blocks and number of points of each block are 185×13, 93×23 respectively. The multiple harmonic transparent acoustic conditions are applied at the inlet and the nonreflecting boundary condition at the outlet to avoid reflection at exit of the transmitted wave, $\boldsymbol{T}$. The amplitude of incident wave, ε is 0.00001. Time step, $\Delta\tau$ is 0.001 and Δf is 0.05. Fig. 2 shows the normalized acoustic pressure $(=p'/\varepsilon=(p-p_0)/\varepsilon)$ contours in the space-

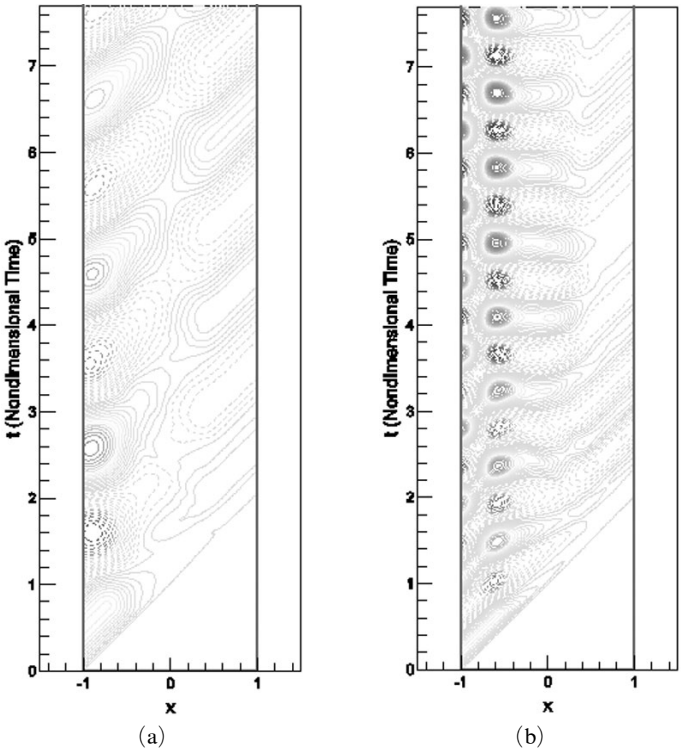

Fig. 2 Normalized acoustic pressure in the space-time domain for a circular expansion chamber silencer without extended inlet/outlet along the symmetric axis ($y=0$) (---- negative value, —— positive value, contour level interval $\Delta p'/\varepsilon=0.1$) (a) $f=0.5$ (b) $f=1.15$

time domain along the symmetric axis ($y=0$) and shows the wave propagation and reflection process. Fig. 2(a) shows the incident wave propagation through the expansion chamber at the speed of sound with the minimum loss. However, (b) shows most part of the incident wave is reflected at the starting ($x=-0.5$) and ending ($x=0.5$) points of an expansion chamber so that the standing wave pattern could be shown in the inlet duct ($x<-0.5$) and the amplitude of transmitted wave is small ($x>0.5$). And the standing wave pattern can be clearly found in the expansion chamber region at the maximum loss frequency, $f=1.15$. Time histories of acoustic pressures at the inlet ($x=-1$) and the outlet ($x=1$) are shown in Fig. 3(a) and TL is shown in (b). The calculated TL has good agreement with semi-analytic results (Munjal, 1987b). Sharp right angle corners at the abrupt area changes make the sharp peak in Fig. 3(b) at f=1.15 in semi-analytic calculation. However in this approach, the numerical wall boundary condition makes sharp right angle corners be a little rounded like the real corners so that the present TL at sharp peak of semi-analytic results is under predicted and has even better agreements with the experimental results, which the next results clearly show.

Next, the circular expansion chamber silencer with extended inlet and outlet as shown in Fig. 4 is analyzed. Grid system consists of 2 blocks and number of points of each block are 222×8, 153×16 respectively. The amplitude of incident wave, ε is 0.00001. Time step, $\Delta\tau$ is 0.001 and Δf is 0.05. Time histories of acoustic pressures at the inlet ($x=-0.734043$) and the outlet ($x=0.734043$) are shown in Fig. 8(a) and TL is shown in (b). The calculated TL has quite good agreement with semi-analytic results (Åbom, 1990) and even better

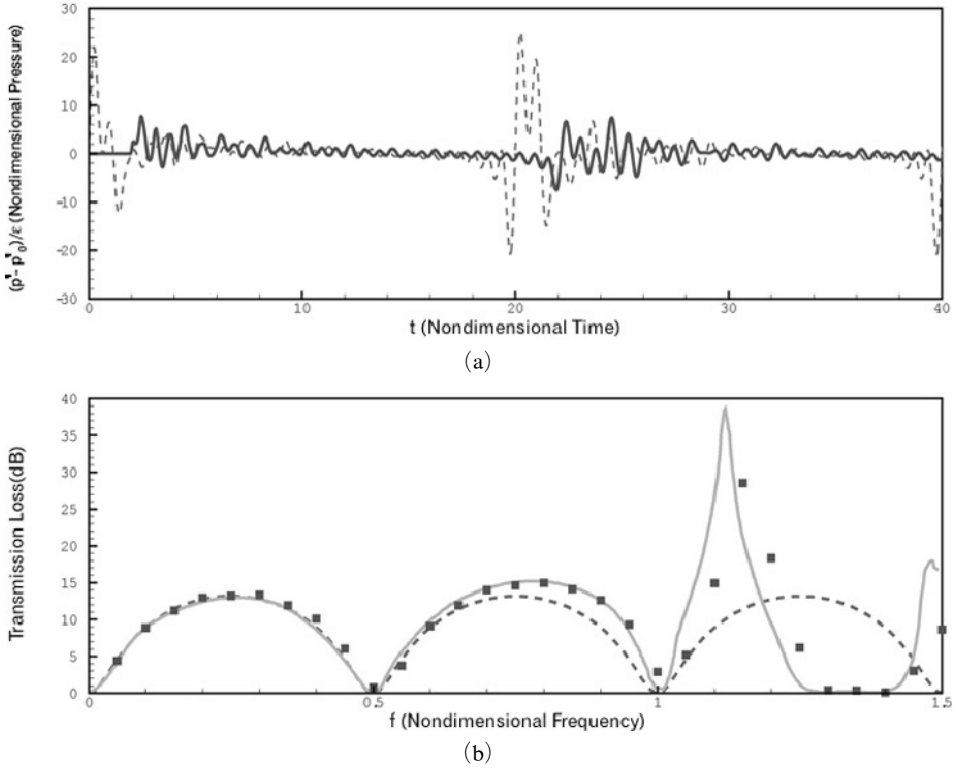

Fig. 3 Time history and transmission loss for a circular expansion chamber silencer without extended inlet/outlet (a) time history of normalized acoustic pressure (---- inlet, —— outlet) (b) transmission loss (---- analytic solution based on the plane wave theory, —— semi-analytic result (Munjal, 1987b), ■ result of the present method)

agreement with experimental results (Åbom, 1990). It could be resulted from that the effect of the finite thickness and rounded tip of the extended edges due to the numerical wall boundary condition makes better present results than semi-analytic results.

3.2 Linear incident wave with mean flow at two different mach numbers

First, we need the steady state solution of the

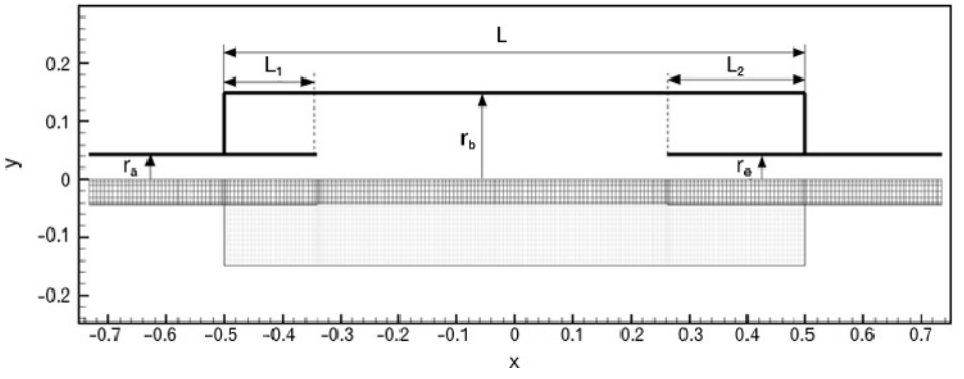

Fig. 4 Computational domain for a circular expansion chamber silencer with extended inlet/outlet (L/r_a= 23.5, L_1/r_a=3.72, L_2/r_a=5.58, r_b/r_a=3.49, r_a/r_e=1)

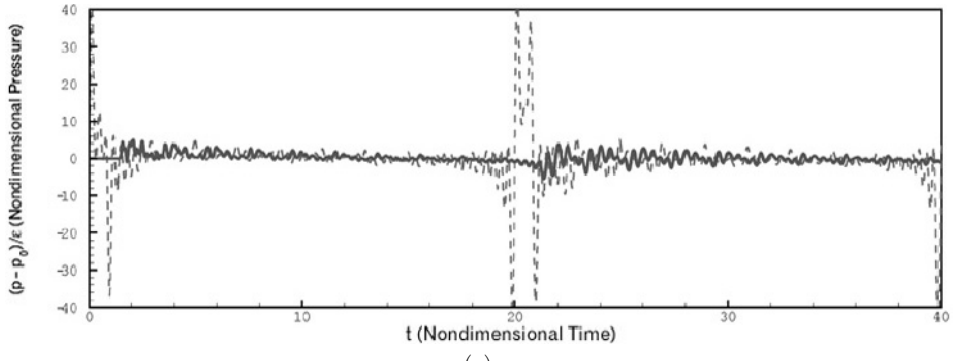

(a)

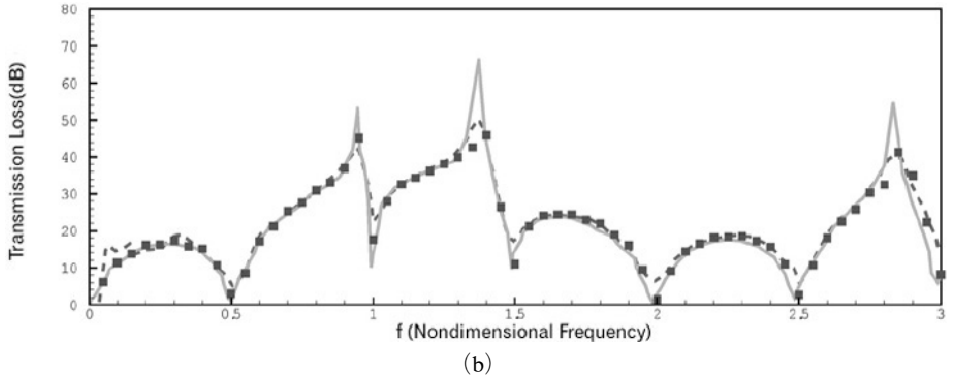

(b)

Fig. 5 Time history and transmission loss for a circular expansion chamber silencer with extended inlet/outlet (a) time history of normalized acoustic pressure (---- inlet, —— outlet) (b) transmission loss (---- experimental result (Åbom, 1990), —— semi-analytic result (Åbom, 1990), ■ result of the present method)

internal flows to consider the mean flow effect in this approach. Then, incident waves are applied to the steady mean flow converged by a machine error to obtain the time history of the transmitted wave. The exponential pipe silencer with slight area change is selected for the benchmark problem as shown in Fig. 6. The radius r is defined as below.

$$r = r_b e^{\{\log(r_a/r_b)(x-x_s)/(x_e-x_s)\}} \tag{12}$$

where x_s and x_e are starting $(x=-0.7)$ and ending $(x=-0.3)$ points of expansion, respectively. Grid points are 201×12. Fig. 6(b) shows the convergence history. The fluctuation of the steady state solution seems to be a machine error. Fig. 6 (c) shows the steady state mean flow pressure contours calculated, using the same numerical method. Fig. 6(d) and (e) show cross flow gradient as well as axial flow gradient of the steady state mean flow which makes the convection and refraction, respectively. Most of semi-analytic and boundary element methods have difficulties to deal with a cross flow gradient effect. One of the advantages of the present method is that it can directly consider the arbitrary flow gradient.

In this case, $\Delta\tau$ is 0.001 and Δf is 0.1. The following three cases are calculated; no mean flow, mean flow Mach number 0.1 and mean flow Mach number 0.3. The amplitude of incident wave, ε is 0.00001. Fig. 7 shows the calculated TL of each case compared with the semi-analytic results (Easwaran and Munjal, 1992). The calculated TL has quite good agreements. In low frequency range, TL seems to be affected by mean flow gradients due to the refraction, especially in the case of mean flow Mach number 0.3. High frequency waves seem to be a little affected by mean flow gradients and expansion chamber due to the small area change.

3.3 Nonlinear incident wave

Finally the nonlinear incident wave case is investigated to check the usefulness of the present approach. We use 0.1 as the amplitude of incident

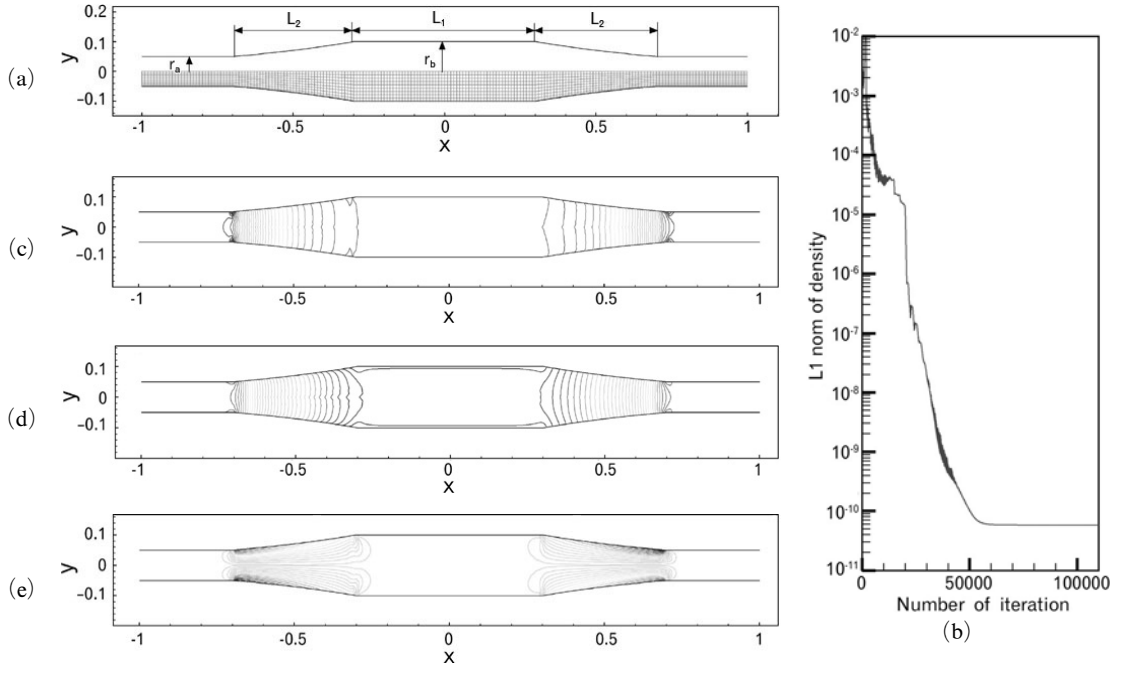

Fig. 6 Grid system and steady state solution of the exponential pipe silencer with mean flow Mach number 0.3 (L_1/L_2=1.5, r_b/r_a=2, L_1/r_a=12) (a) grid system (b) convergence history (c) pressure contours (d) u speed (x direction) contours (e) v speed (y direction) contours

wave, ε to see the nonlinear effect clearly. Previous study (Kim and Lee, 2001) showed the noise level near a valve of internal combustion engine is around 10 to 15% of the ambient pressure. It is known (Witham, 1974) that a sinusoidal finite wave becomes the periodic N wave as it propagates along the pipe due to the nonlinear hyperbolic characteristics. Most of linearized approaches have difficulties to simulate nonlinear wave propagation. The length of inlet duct is extended sufficiently to produce the periodic weak shock, i.e. N waves. We select the insertion loss (IL) as a major parameter to analyze the sound attenuation characteristics of the silencer, because TL is inappropriate for the performance representation in case of N waves which contain many higher harmonic components even for single harmonic incidence. Single harmonic acoustic source is applied rather than multiple harmonics because it is easy to investigate the frequency effect. The IL is defined as below

$$IL=10\log_{10}(|\boldsymbol{T}_{straight}|/|T_{silencer}|)^2 \qquad (13)$$

where $\boldsymbol{T}_{straight}$ and $T_{silencer}$ are peak amplitudes of the transmitted waves without and with silencer at the corresponding frequency. Grid points are 401×12 and $\Delta\tau$ is 0.001.

Figure 8 shows the computational domain and pressure contours of two different frequency cases, i.e. 0.5 and 0.75 that are one of minimum and maximum TL frequencies for linear incident wave, respectively. Fig. 8(b) and (c) show the weak shock formed clearly and higher order mode in the expansion chamber. Fig. 9 shows pressure contours of $f=0.5$ case in the space-time domain. Fig. 9(a) shows pressure contours of a straight pipe case. The mechanism of the periodic N wave formation is clearly shown and nonreflecting boundary condition is working well even for the weak shock. Fig. 10(a) also shows time histories of the periodic N wave. Fig. 9(b) and (c) show pressure contours of an exponential pipe silencer case. The stationary state in this case could be achieved after $t=200$ because it spends long time that all transient waves in the duct propagate outside the computational domain. Contours of stationary state solution show that the considerable amount of incident waves are reflected at $x\approx-0.5$ and the reflected wave, $\boldsymbol{R}$ becomes the weak shock as it propagates backward. So, a periodic abrupt change can be found in acoustic pressure time history at inlet as shown in Fig. 10(b). The amplitude of transmitted wave is also quite large and it looks there is a little effect for sound attenuation. However, the calculated IL as shown in Fig. 10(c) explains that the component of $f=0.5$ is transmitted with minimum loss, however higher harmonics have considerable losses so that the transmitted wave recovers the sinusoidal pattern rather than N pattern. Basically, similar phenomena can be observed in $f=0.75$ case. However, the insertion loss is smaller than that of $f=0.5$ because the pressure time histories at the outlet in Fig. 11(b) show nearly weak shock due to lots of transmission of higher harmonics. We can

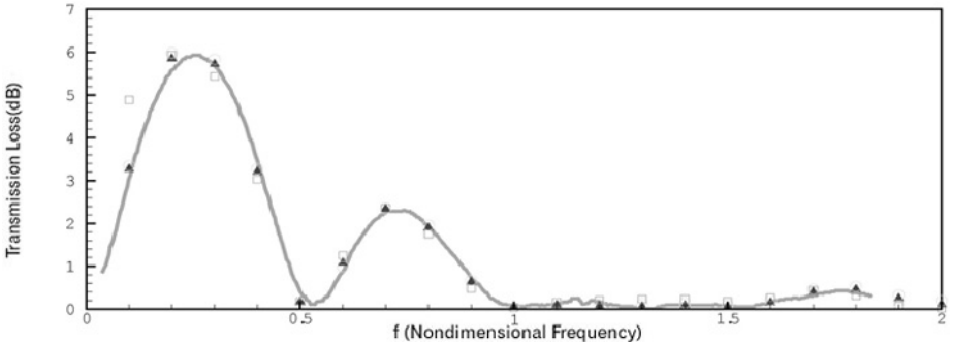

Fig. 7 Transmission loss of an exponential pipe silencer (—— Easwaran and Munjal (1992) (mean flow Mach number 0.1), ▲ no mean flow, ○ mean flow Mach number 0.1, □ mean flow Mach number 0.3)

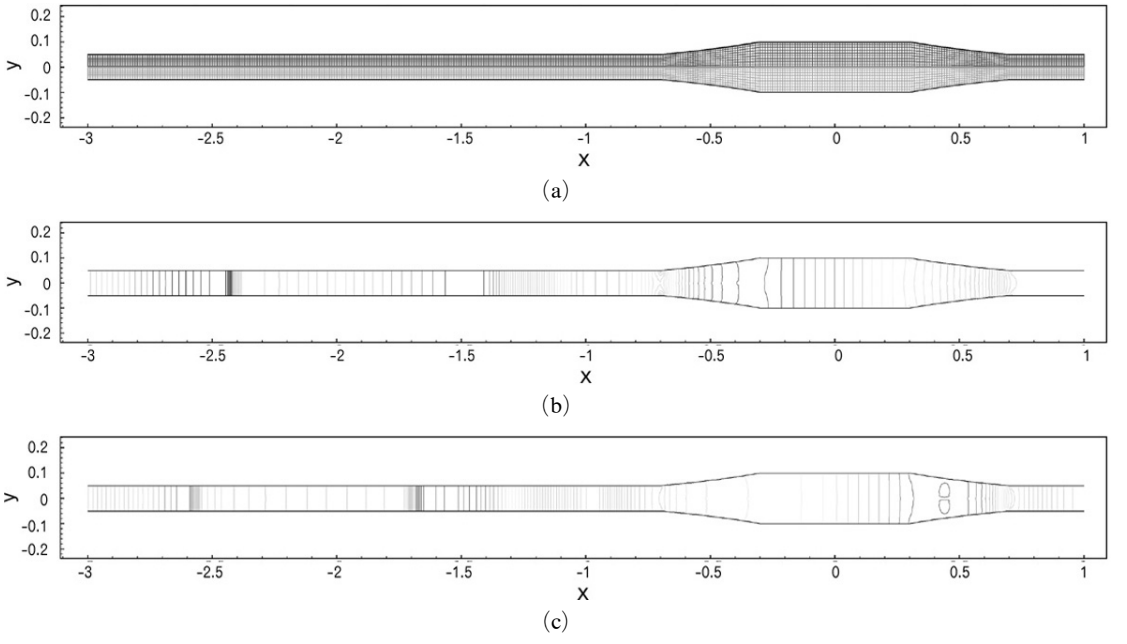

Fig. 8 Grid system and pressure contours on the center section for an exponential pipe silencer (contour level interval $\Delta p'/\varepsilon=0.1$) (a) grid system and computational domain (b) pressure contours of $f=0.5$ case (at $t=250$) (b) pressure contours of $f=0.75$ case (at $t=160$)

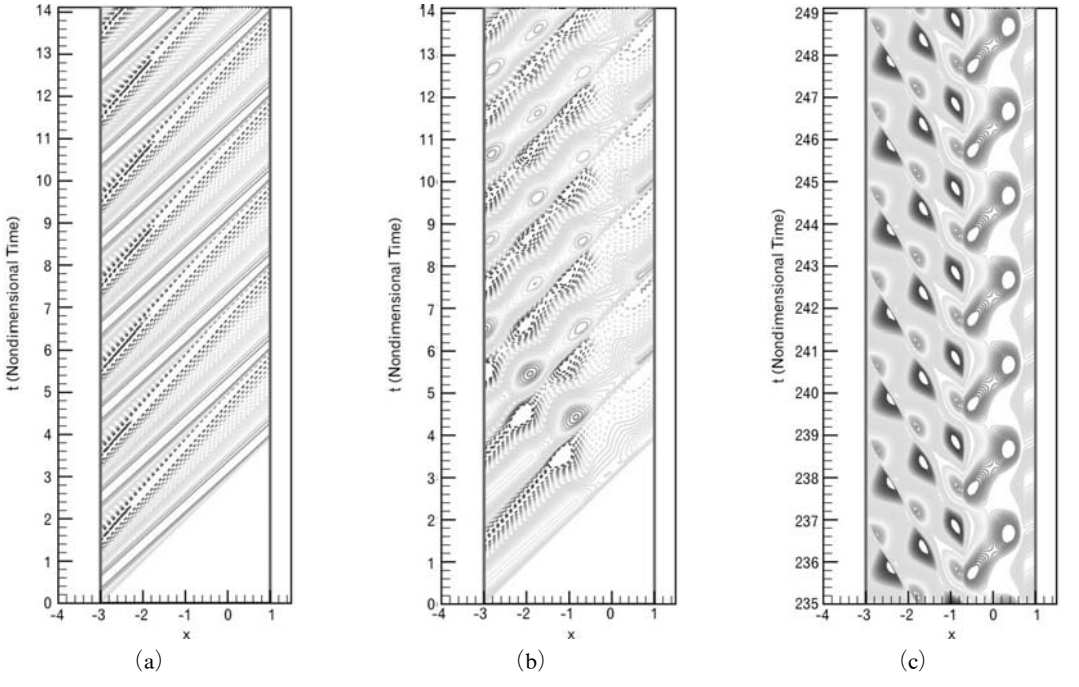

Fig. 9 Normalized acoustic pressure contours in the space–time domain for a circular straight pipe compared with those of an exponential pipe silencer along the symmetric axis ($y=0$) ($f=0.5$, $\varepsilon=0.1$, contour level interval $\Delta p'/\varepsilon=0.1$) (---- negative value, —— positive value) (a) stationary state in straight pipe (b) transient state in exponential pipe silencer (c) stationary state in exponential pipe silencer

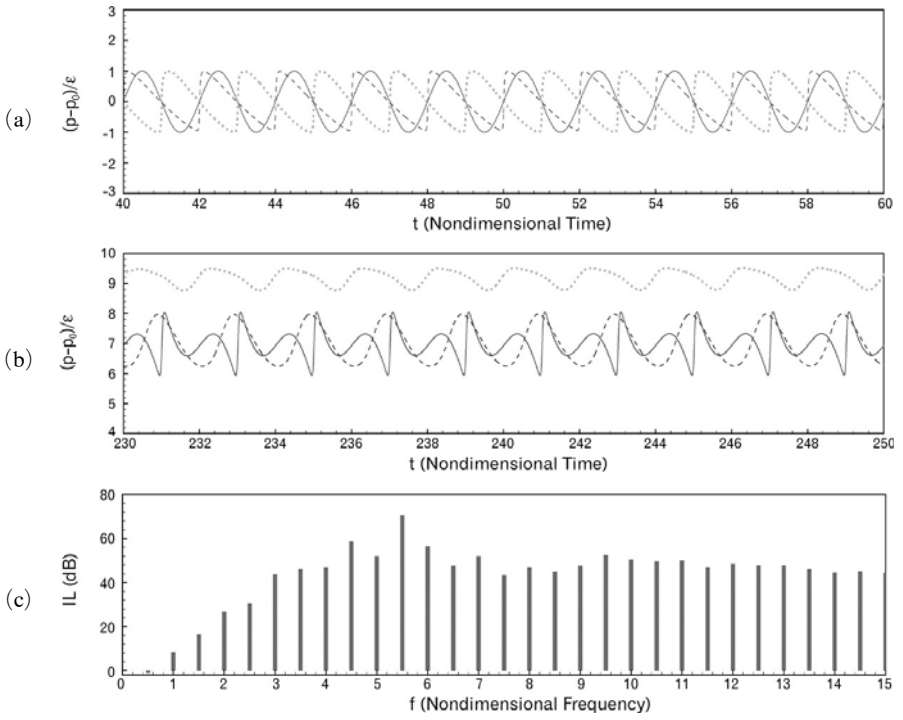

Fig. 10 Time histories of normalized acoustic pressure at $y=0$ ($f=0.5$, $\varepsilon=0.1$) (—— inlet, ···· center of expansion chamber, ---- outlet) (a) straight pipe (b) exponential pipe silencer (c) insertion loss

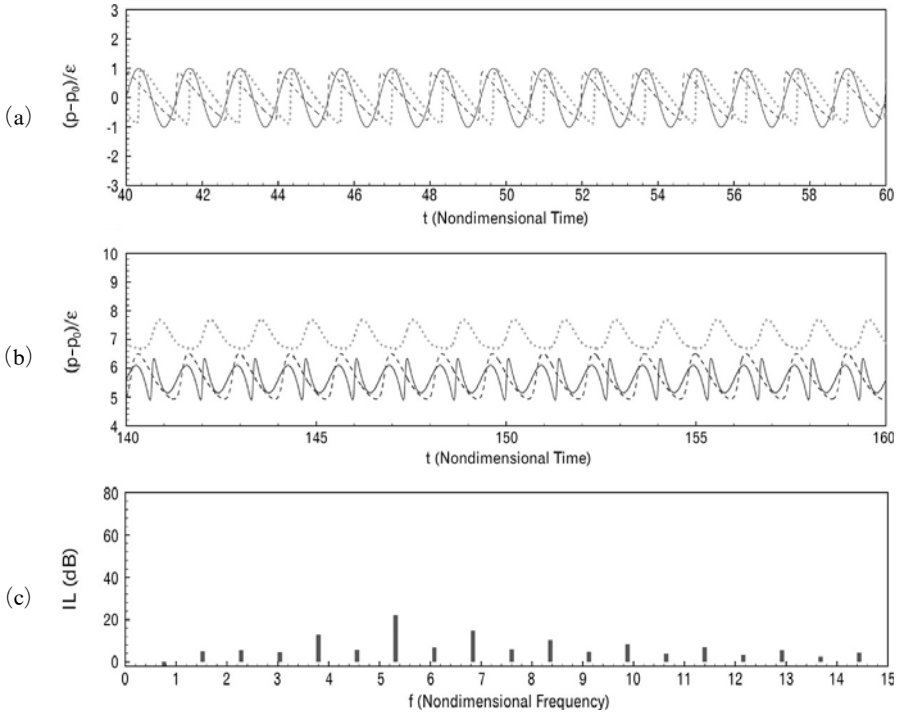

Fig. 11 Time histories of normalized acoustic pressure at $y=0$ ($f=0.75$, $\varepsilon=0.1$) (—— inlet, ···· center of expansion chamber, ---- outlet) (a) straight pipe (b) exponential pipe silencer (c) insertion loss

not conclude yet a reactive silencer can reduce the periodic weak shock noise effectively, however we can say the present approach can be an analysis tool for such a kind of silencer from this study.

4. Conclusions

The time accurate finite difference method for axisymmertic Euler equations is applied to the performance prediction of a silencer. The following conclusions have been drawn from this study :

(1) The silencer performance prediction procedure, using a time accurate finite difference method of Euler equations, is established. It can be reasonably efficient using a multiple transparent acoustic source conditions in case of linear incident waves.

(2) The prediction accuracy of the present method is validated in two different shapes of circular expansion chamber, and two different mean flow conditions in the exponential pipe silencer. Especially, the results of present method have better agreements with the experimental results than semi-analytic results.

(3) The present method clearly captures the N wave in nonlinear wave propagation without numerical oscillation errors, and can predict the silencer performance in terms of an insertion loss.

References

Åbom, M., 1990, "Derivation of Four-Pole Parameters Including Higher Order Mode Effects for Expansion Chamber Mufflers with Extended Inlet and Outlet," *Journal of Sound and Vibration*, Vol. 137, pp. 403～418.

Easwaran, V. and Munjal, M. L., 1992, "Plane Wave Analysis of Conical and Exponential Pipes with Incompressible Mean Flow," *Journal of Sound and Vibration*, Vol. 152, pp. 73～93.

Hirsch, C., 1990, "Numerical Computation of Internal and External Flows," John Wiley & Sons, pp. 408～594.

Hwang, C. and Lee, D. J., 1995, "A Transparent Acoustic Source Condition Applied to the Euler Equations," *American Institute of Aeronautics and Astronautics Journal*, Vol. 33, pp. 1736～1738.

Ji, Z., Ma, Q. and Zhang, Z., 1994, "Application of the Boundary Element Method to Predicting Acoustic Performance of Expansion Chamber Mufflers with Mean Flow," *Journal of Sound and Vibration*, Vol. 173, pp. 57～71.

Ju, H. D. and Lee, S. B., 2005, "Transmission Loss Estimation of Three Dimensional Silencers with Perforated Internal Structures Using Multi-domain BEM," *Journal of Mechanical Science and Technology*, Vol. 19, pp. 1568～1575.

Kim, Y. H., Choi, J. W. and Lim, B. D., 1990, "Acoustic Characteristics of an Expansion Chamber with Constant Mass Flow and Steady Temperature Gradient (Theory and Numerical Simulation)," *Journal of Vibration and Acoustics, Transactions of the American Society of Mechanical Engineering*, Vol. 112, pp. 460～467.

Kim, Y. S. and Lee, D. J., 2001, "Numerical Analysis of Internal Combustion Engine Intake Noise with a Moving Piston and a Valve," *Journal of Sound and Vibration*, Vol. 241, pp. 895～912.

Munjal, M. L., 1987a, "Acoustics of Ducts and Mufflers," John Wiley & Sons

Munjal, M. L., 1987b, "A Simple Numerical Method for Three-Dimensional Analysis of Simple Expansion Chamber Mufflers of Rectangular as well as Circular Cross-Section with a Stationary Medium," *Journal of Sound and Vibration*, Vol. 116, pp. 71～88.

Thompson, K. W., 1990, "Time Dependent Boundary Conditions for Hyperbolic Systems, II," *Journal of Computational Physics*, Vol. 89, pp. 439～461.

Tsuji, T., Tsuchiya, T. and Kagawa, Y., 2002, "Finite Element and Boundary Element Modeling for the Acoustic Wave Transmission in Mean Flow Medium," *Journal of Sound and Vibration*, Vol. 255, pp. 849～866.

Witham, G. B., 1974, "Linear and Nonlinear Waves," John Wiley & Sons, pp. 42～52.